# Converted waves: properties and 3D survey design

*Gijs J.O. Vermeer, 3DSymSam - Geophysical Advice*

**Summary**

3D survey design for converted waves should take their specific properties into account. In the first part of this paper properties of PS-waves are investigated in various minimal data sets (3D single-fold basic subsets of acquisition geometry). The apparent velocities in the 3D receiver gather are much larger than in the 3D shot gather. The cross-spread shows significant asymmetry. Illumination and resolution depend strongly on the minimal data set. In the second part the consequences of these properties for 3D survey design are reviewed. It turns out that parallel geometry is a better choice than orthogonal geometry, unless azimuth-dependent effects need be analyzed. Receiver sampling is preferably denser than shot sampling.

**Introduction**

Only a few papers seem to have been published on the design of 3C 3D seismic surveys (Lawton, 1995, Cordsen and Lawton, 1996). These papers deal mostly with binning issues, in association with the asymmetric illumination by PS-waves. In my opinion, binning issues are better left to processing, in particular when spatial interpolation to neighboring bin centers (Herrmann et al., 1997, Beasley and Mobley, 1997) becomes more generally accepted.

Yet, the asymmetric illumination by PS-waves is the major reason that the design of 3D surveys for converted waves is more complicated than for P- or S-waves. This paper starts with an analysis of the properties of the PS-wavefield in various minimal data sets, followed by an expansion of the design techniques developed for P-wave acquisition (Vermeer, 1998, 1999) to PS-waves.

**Properties of the PS-wavefield**

In the following a constant velocity isotropic medium is used as a basis for the investigations.

*Traveltime surfaces and apparent velocity-* The traveltime for a PS reflection as a function of offset is controlled by Snell's law (see Figure 1):

$$\frac{\sin\alpha}{V_s} = \frac{\sin\beta}{V_p}, \qquad (1)$$

The asymmetry between the P- and the S-leg of the raypaths leads to asymmetrical traveltime curves, except for a horizontal reflector.

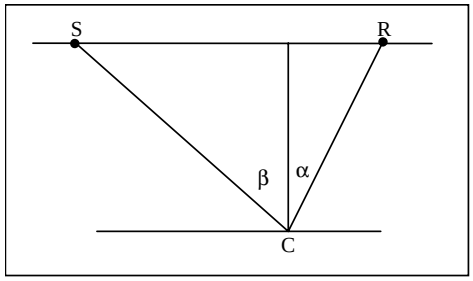


Fig. 1 PS reflection at a horizontal reflector

The diffraction traveltime is different between common-shot diffractions and common-receiver diffractions. In the common shot the diffraction is much steeper because the slow $V_s$ determines the change in traveltime. This is illustrated in Figure 2a. The corresponding apparent velocities (as measured in the surface coordinate systems) are plotted in Figure 2b. All apparent velocities seem to be controlled by the P-wave velocity only, except the PS-diffraction in the common shot, which has very low apparent velocities tending towards the S-wave velocity.

The asymmetry in PS acquisition becomes more apparent for

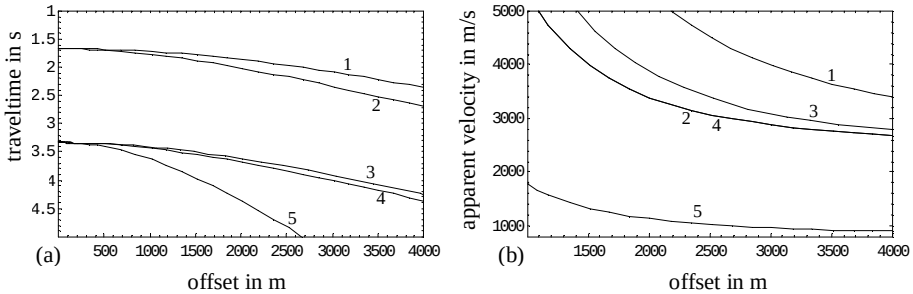


Fig. 2 Traveltime curves (a) and apparent velocity (b) for PP and PS reflections and diffractions in constant velocity medium. $V_p$ =2400 m/s, $V_s$ =800 m/s, depth of reflector is 2000 m, diffractor is at (0, 0, 2000). 1= PP-reflection, 2 = PP-diffraction, 3 = PS-reflection, 4 = PS-diffraction in common receiver, 5 = PS-diffraction in common shot.

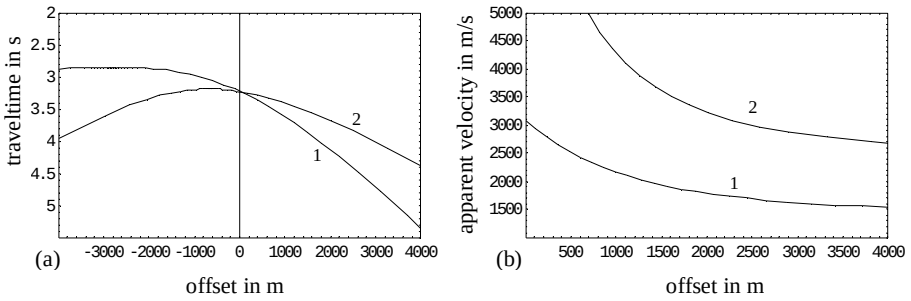


Fig. 3 PS-reflection in common shot (1) and common receiver (2) for 15° dip. Depth of reflector at position of shot, receiver is 2000 m. (a) traveltimes, (b) apparent velocity. The common shot has the steepest curve and the smallest apparent velocity.

dipping reflectors. This is illustrated for a reflector with 15° dip in Figure 3. Note that the common shot sees the steepest reflection time curve with an apparent velocity smaller than the P-wave velocity.

Different acquisition geometries can be compared using the diffraction traveltimes curves in their minimal data sets (Vermeer, 1998). Figure 4 shows contour plots of those curves for the common receiver, the common shot, the common-offset gather with constant azimuth (COA) and the cross-spread. In the common shot the S-wave velocity determines the slopes of the curves, whereas in the common receiver the P-wave velocity determines the slopes. The curves in the common-offset gather have some intermediate slope. This can be understood by realizing that the apparent velocity $V_a$ in the zero-offset gather would tend to $1/V_a = 1/V_p + 1/V_s$ for large distances from the scatterer. Note that - unlike a PP-diffraction - the apex of the PS-traveltime surface is offset from the diffractor position. The cross-spread shows a mixed behavior: steep flanks in the in-line (receiver) direction and gentle slopes in the cross-line (source) direction.

*Illumination*- In P-wave acquisition the midpoint coverage is the same as subsurface coverage of horizontal reflectors. Therefore, fold-of-coverage is fairly representative for illumination fold, even for areas with gentle dips. This is quite different for PS-wave acquisition due to the asymmetry in the raypaths. Figure 5 shows a comparison of the midpoint area of three different minimal data sets with the illumination areas of a horizontal reflector for $V_p / V_s = 1.5$ and $V_p / V_s = 3$. The midpoint area is the 2000 x 2000 m square in the figure. It also represents the illumination area for a PP-reflection. The other curves represent the conversion point curves corresponding to the midpoints along the outline of the square. The cross-spread shows asymmetry: the illumination area is wider in the in-line direction and narrower in the cross-line direction than the midpoint area. The 3D shot has the largest illumination areas and the 3D receiver the smallest.

For dipping reflectors the illumination areas will shift updip. The illumination area of a COA gather is not shown in Figure 5 to prevent clutter. It would be a square illumination area with the same size as the midpoint area, but shifted towards the receivers.

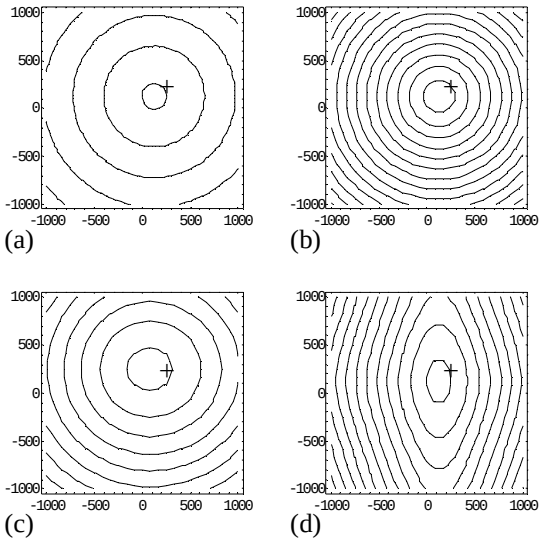


Fig. 4 Diffraction traveltime contours for various minimal data sets plotted in midpoint coordinates. Contour interval is 250 ms. Position of diffractor in (250, 250, 500) is indicated by a "+", $V_p$ = 2400 m/s, $V_s$ = 800 m/s, (a) common receiver, (b) common shot, (c) COA gather (600 m), (d) cross-spread.

*Resolution*- In Vermeer (1999) a comparison is made of the PP-wavenumber spectra of different minimal data sets for a single diffractor. The spectra were computed using Beylkin's formula, which allows computation of the wavenumber range for a given minimal data set and velocity model. The same formula can be used to compute the PS-wavenumber spectra.

For the PS-situation and constant velocities $V_p$ and $V_s$ Beylkin's formula can be written as

$$\mathbf{k} = f\left(\frac{\nabla_x d_s}{V_p} + \frac{\nabla_x d_r}{V_s}\right), \qquad (2)$$

where **k** is the wavenumber vector, $f$ is frequency, $d_s$ is raypath from shot to conversion point, $d_r$ is raypath from conversion

point to receiver and $\nabla_x$ is the derivative with respect to the subsurface point **x** being investigated. As compared to the formula for P-waves, $V_s$ in this formula has replaced $V_p$. The small $V_s$ tends to increase the range of wavenumbers as illustrated in Figures 6 and 7. As Figure 6 clearly shows, there is a considerable difference between the resolution obtainable with a 3D shot and a 3D receiver, whereas in PP-acquisition their resolution would be the same. The cross-spread spectrum has a hammock shape, indicative of the asymmetry between in-line and cross-line direction.

Figure 7 shows the projections on the horizontal plane of the PS-wavenumber spectra of various minimal data sets for $V_p$ / $V_s$ = 1, 1.5 and 3 and constant $V_p$ = 2400 m/s. Notable is the invariance of the 3D receiver resolution to $V_p$ / $V_s$. This is because $V_p$ is kept constant, whereas the $V_p$ -leg of the raypath fully determines the resolution in the 3D receiver. The asymmetry in the cross-spread leads to less resolution in the cross-line (source) direction than in the in-line direction. There is also asymmetry in the resolution of the COA gathers. The resolution is best for the downdip shooting part of the wavefield (positive *x*, *y* map onto negative $k_x$, $k_y$, hence a shot-receiver combination with positive coordinates, source to the left of the receiver, maps to negative *k*).

Figure 7 shows that - except for the 3D receiver gather - the resolution of PS data is better than the resolution of PP data *for the same frequency*. In practice, PS data tend to have lower maximum frequency than PP data, thus reducing or even losing the relative advantage.

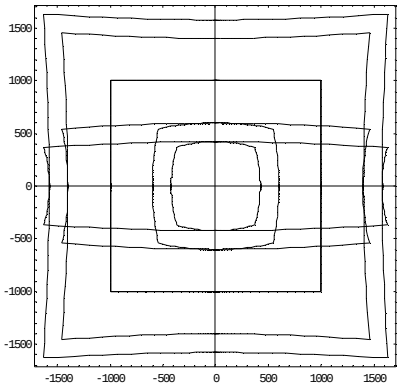


Fig. 5 Illumination areas for the 3D shot (the two widest curves), the 3D receiver (the two curves in the center), and the cross-spread (the asymmetric curves) for $V_p$ / $V_s$ = 3 and $V_p$ / $V_s$ = 1.5. The 2000 x 2000 m square represents the midpoint area of the three minimal data sets. The depth of the horizontal reflector is 2000 m.

### 3D survey design for PS-waves

*Choice of geometry*- Very often the choice of geometry will be dictated by circumstances such as available budget. On land, this tends to lead to orthogonal geometry or some

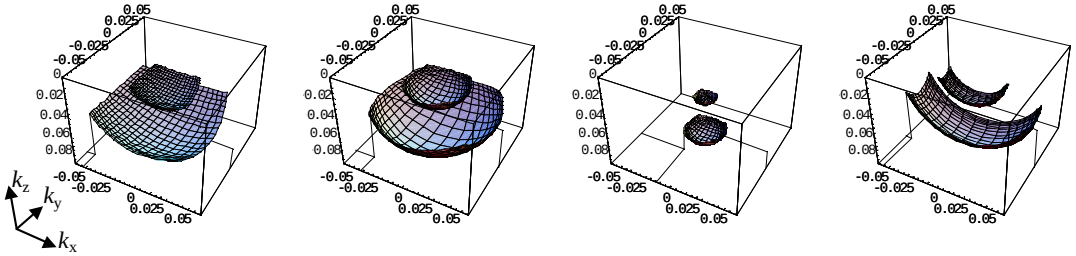


Fig. 6 PS-wavenumber spectra for four minimal data sets, $V_p$ / $V_s$ = 3. All data sets have the same 1000 x 1000 m midpoint area, with the diffractor in the centre. The surfaces correspond to constant input frequencies 25 Hz (upper surfaces) and 50 Hz. From left to right: 600 m COA gather, 3D shot, 3D receiver and cross-spread.

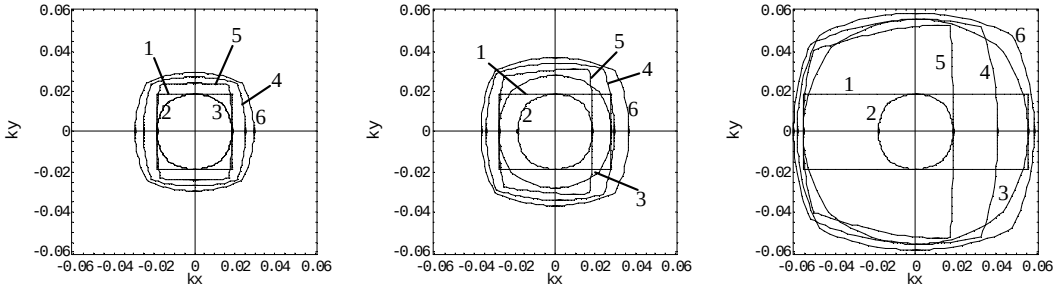


Fig. 7 Coverage in horizontal PS-wavenumber domain by six different minimal data sets with the same 1000 x 1000 m midpoint area for $V_p$ = 2400 m/s and $V_s$ = 2400 (left), 1600 (center) and 800 (right) m/s. 1= cross-spread, 2 = 3D receiver, 3 = 3D shot, 4 = 600 m COA gather, 5 = 1000 m COA gather, 6 = zero offset. The zero-offset is hypothetical, as PS-waves have zero amplitude for zero-offset.

derivative thereof (e.g. slanted shotlines), for marine streamer acquisition to parallel geometry and for OBC work to orthogonal geometry. Nevertheless, geophysical requirements should play a role as well, and need to be properly understood. In the first part of this paper we have seen that illumination and resolution both depend strongly on which minimal data set is used, hence on acquisition geometry.

As far as illumination is concerned, COA gathers can obtain the most regular illumination. Just as for P-wave acquisition the illumination area is not very different from the midpoint area and there are no internal boundaries: the illumination area is continuous throughout. Resolution is better for downdip than for updip shooting. This problem can be taken care of by center-spread acquisition.

On the other hand, the illumination area of a cross-spread is asymmetrical and depends strongly on $V_p$ / $V_s$. Moreover, resolution of cross-line dips is inferior to in-line dips. These are pretty serious disadvantages of this geometry. Hence, parallel geometry tends to be better geometry for PS acquisition than orthogonal or any other crossed-array geometry. An important advantage of orthogonal geometry is that it allows analysis of azimuth-dependent effects such as fracture orientation. This would require two orthogonal acquisition passes with parallel geometry.

The use of areal geometry tends to be practical only with 3D receiver gathers and not with 3D shot gathers. Unfortunately, the illumination area of a 3D receiver is relatively small, whereas resolution tends to be lower than achievable with PP-data. This requires a relatively high density of 4C receivers. This geometry is most suitable for analysis of azimuth-dependent effects. Experimental results of a 3D/4C areal geometry are reported in Ridyard et al. (1998).

*Sampling*- The sampling interval in any spatial domain is determined by the smallest apparent velocity and the largest frequency. This means that for equal maximum frequency the sampling of the receivers in a common shot depends on the S-wave velocity, whereas the sampling of the shots can be the same as for P-wave acquisition. In the cross-spread this leads to asymmetric sampling requirements.

Sampling parallel geometry is of special interest. Here again, proper sampling of the field data requires a smaller sampling interval for the receivers than for the shots. The required midpoint sampling of the COA gather (see Figure 4) depends on the harmonic average of P-wave and S-wave velocities, hence seems to be less strict than in the 3D-shot gather. However, to realize the required midpoint sampling for each offset, shot and receiver sampling intervals would have to be equal to the required midpoint sampling interval, because each offset only occurs at every other midpoint. Therefore, proper sampling of COA gathers can best be achieved by interpolation of properly sampled shot and receiver gathers.

*Illumination and fold*- For parallel geometry, considerations on fold and illumination are similar as for P-wave acquisition, although it is important to choose center-spread acquisition. Positive and negative offsets illuminate different subsurface points.

For orthogonal geometry, the cross-line illumination fold is smaller than cross-line fold-of-coverage and depends on $V_p$ / $V_s$. There is very little one can do to ensure regular subsurface illumination, but the minimum requirement is that the illumination areas of adjacent receiver lines are partially overlapping. This may have to be tested with raytracing. Usually, it will be sufficient (for not too complex geology) to compute the outline of the illumination areas only, because only there discontinuities in illumination are to be expected. Inside the outline the illumination fold is one throughout, *independent of binsize*. This reduces the required raytracing effort considerably. The receiver line spacing may have to be reduced to increase cross-line illumination fold.

## Conclusions

Designing 3D surveys for PS-waves needs to take the asymmetric raypath and illumination into account. Orthogonal geometry leads inevitably to irregular illumination, which requires special attention in processing, whereas parallel geometry may achieve an illumination which is as regular as for P-wave acquisition. On the other hand, parallel geometry is not suitable for analysis of azimuth-dependent effects, unless two acquisition passes are carried out. At the end of the day, the sampling requirements of both P-wave and PS-wave acquisition have to be harmonized, taking into account differences in maximum frequency between the two wave types.

## References

Beasley, C.J., and Mobley, E., 1997, Spatial dealiasing of 3-D DMO: 67th Ann. Internat. Mtg., Soc. Expl. Geophys., Expanded Abstracts, paper SP3.7

Cordsen, A., and Lawton, D.C., 1996, Designing 3-component 3-D seismic surveys: 66th Ann. Internat. Mtg., Soc. Expl. Geophys., Expanded Abstracts, paper Acq3.7.

Herrmann, P., David, B., and Suaudeau, E., 1997, DMO weighting and interpolation: EAGE Extended Abstracts, Volume 1, paper A050.

Lawton, D., 1995, Converted-wave 3-D surveys: design strategies and pitfalls: Can. Soc. Expl. Geophys., Ann. Mtg. Abstracts, 69-70.

Ridyard, D., Maxwell, P., Fisseler, G., and Roche, S., 1998, A novel approach to cost effective 4C/4D - the Teal South experiment: EAGE Extended Abstracts, Volume 1, paper 2-01.

Vermeer, G.J.O., 1998, 3-D symmetric sampling: Geophysics, **63**, 1629-1647.

Vermeer, G.J.O., 1999, Factors affecting spatial resolution: Geophysics, 64, 942-953.